



Contents lists available at ScienceDirect

Journal of Inorganic Biochemistry

journal homepage: www.elsevier.com/locate/jinorgbio

Synthesis and antimicrobial activity of tetradentate ligands bearing hydrazone and/or thiosemicarbazone motifs and their diorganotin(IV) complexes

Cristina González-García^{a,1}, Alejandro Mata^a, Franca Zani^{b,*}, M. Antonia Mendiola^a, Elena López-Torres^{a,*}

^a Departamento de Química Inorgánica, Universidad Autónoma de Madrid, C/ Francisco Tomás y Valiente 7, 28049 Madrid, Spain

^b Dipartimento di Farmacia, Università degli Studi di Parma, Parco Area delle Scienze 27/A, 43124 Parma, Italy

ARTICLE INFO

Article history:

Received 16 March 2016

Received in revised form 27 June 2016

Accepted 7 July 2016

Available online xxxx

Keywords:

Thiosemicarbazones

Hydrazones

Diorganotin(IV) complexes

X-ray diffraction

¹¹⁹Sn NMR

Antimicrobial activity

ABSTRACT

Four novel ligands derived from 2,3-butanedione have been synthesized, two dissymmetric thiosemicarbazone/3-hydroxy-2-naphthohydrazone ligands, **H₂L¹** (bearing 4-isopropyl-3-thiosemicarbazone) and **H₂L²** (containing 4-cyclohexyl-3-thiosemicarbazone) and the symmetric **H₂L³**, diacetyl bis(3-hydroxy-2-naphthohydrazone), and **H₂L⁴**, diacetyl bis(4-cyclohexyl-3-thiosemicarbazone). Their reactivity with SnR₂Cl₂ (R = methyl, *n*-butyl and phenyl) was explored and the resulting complexes were characterized by elemental analysis, molar conductivity, mass spectrometry, IR, ¹H, ¹³C and ¹¹⁹Sn NMR and seven of them also by single crystal X-ray diffraction. The results showed that the reactivity of the dissymmetric ligands is strongly different and while the cyclohexyl derivative is very stable, with isopropyl easily undergoes a symmetrization reaction to yield the corresponding symmetric ligands. The antimicrobial activity of the ligands and the corresponding diorganotin(IV) complexes was investigated *in vitro* against seven species of microorganisms and minimum inhibitory concentrations (MICs) were determined. The results showed that the ligand **H₂L²** and several of its derivatives, together with methyl and phenyl complexes of **H₂L¹**, have the ability of inhibiting the growth of tested bacteria and fungi to different extents. *Bacillus subtilis* and *Staphylococcus aureus* Gram positive strains were the most sensitive microorganisms.

© 2016 Elsevier Inc. All rights reserved.

1. Introduction

The synthesis of hydrazone and thiosemicarbazone complexes have received much attention due to their fascinating structural versatility [1–6] combined with their relevant potential therapeutic activity, such as antitumor, antiviral, antiprotazoal, antibacterial or antifungal agents [7–12]. Therefore, the synthesis of mixed ligands containing both thiosemicarbazone and hydrazone functions is an interesting topic to pursue, although their synthesis is usually hampered by several synthetic problems and an exhaustive control of the reactions conditions must be carried out [13,14]. Concerning to the bioactivity, in many cases the complexes display higher activity than the parent ligands, suggesting that complexation can be an interesting strategy of dose reduction and can also circumvent some side effects [15,16]. This activity is believed to be related to their ability to form stable complexes with a

wide range of metal ions which is increased in the case of ligands bearing two of these thiosemicarbazone/hydrazone functions.

On the other hand, organotin(IV) complexes have been widely investigated because of their structural diversity and biological activity, for example as bactericides, fungicides, acaricides, antifouling and anti-tumor agents [17–27]. According to the literature, the biological properties of organotin(IV) complexes depend on the coordination number of the tin atom, the number and nature of the organic groups as well as on the donor system provided by the ligand. Therefore, any modification made in any of these factors could modulate the complex activity.

The discovery of new antimicrobial substances is of considerable biological importance, owing to the dramatic increase in bacterial and fungal resistance observed in the last decades [28–30]. Hence and as continuation of our studies about organotin(IV) complexes with hydrazone ligands endowed with antimicrobial activity [31,32], we have designed two new tetradentate ligands containing two thiosemicarbazone or hydrazone moieties and two dissymmetric bis(thiosemicarbazone/hydrazone) donors, as well as their complexes with SnR₂Cl₂ (R = Me, *n*-Bu, Ph) and SnL₄. The *in vitro* antimicrobial potency of the ligands and their corresponding diorganotin(IV) complexes was evaluated against various strains of bacteria and fungi. For

* Corresponding authors.

E-mail addresses: franca.zani@unipr.it (F. Zani), antonia.mendiola@uam.es (M.A. Mendiola), elena.lopez@uam.es (E. López-Torres).

¹ Present address: Laboratorio de Tecnología de Polímeros, Universidad Rey Juan Carlos, C/ Tulipán s/n, 28933 Madrid, Spain.

comparison purpose, a similar investigation was performed on tin parent compounds SnMe_2Cl_2 , SnBu_2Cl_2 , SnPh_2Cl_2 and SnI_4 .

2. Experimental

2.1. Measurements

Microanalyses were carried out using a LECO CHNS-932 Elemental Analyzer. IR spectra in the $4000\text{--}400\text{ cm}^{-1}$ range were recorded as KBr pellets on a Jasco FT/IR-410 spectrophotometer. The ESI mass spectra in positive mode were recorded on a Q-STAR PULSAR I instrument using a hybrid analyzer QTOF (Quadrupole time-of-flight). Molar conductivity was measured using a freshly prepared DMF or acetone solution (ca. 10^{-3} M) at 25°C with a Crison EC-Meter BASIC 30+ instrument. ^1H , ^{13}C and ^{119}Sn NMR spectra were recorded on a spectrometer Bruker AVIII HD-300 MHz using $\text{DMSO-}d_6$ or CDCl_3 as solvent and TMS (^1H and ^{13}C) or SnMe_4 (^{119}Sn) as internal reference. ^{119}Sn CP/MAS NMR spectra were recorded at 298 K in a Bruker AV400WB spectrometer equipped with a 4 mm MAS (magic-angle spinning) NMR probe and obtained using a cross-polarization pulse sequence using spinning rates of 10–14 KHz, pulse delays of 30 s, contact times of 8 ms and two-pulse phase-modulated high power proton decoupling. Chemical shifts are reported relative to SnMe_4 , using tin(IV) oxide as a secondary reference.

2.2. Synthesis of the compounds

All the chemicals were purchased from standard commercial sources and used as received.

2.2.1. 4-Isopropyl-3-thiosemicarbazide, $i\text{PrTSC}$

Over a solution of 10.0 mL (93.7 mmol) of isopropylisothiocyanate in 50 mL of diethyl ether cooled in an ice bath, 4.5 mL (93.70 mmol) of monohydrated hydrazine was added dropwise and the mixture was stirred for an hour. The white precipitated formed was filtered off, washed with diethyl ether and vacuum dried (11.78 g, 94%). ^1H NMR ($\text{DMSO-}d_6$) δ 8.48 (1H, s, NH), 7.45 (1H, d, $^3J = 8.6\text{ Hz}$, NH- $i\text{Pr}$), 4.40 (2H, s, NH_2), 4.35 (1H, m, CH), 1.11 (6H, d, $^3J = 6.6\text{ Hz}$, CH_3).

2.2.2. 4-Cyclohexyl-3-thiosemicarbazide, ChTSC

0.71 mL (14.80 mmol) of monohydrated hydrazine was added dropwise over a solution of 2.00 g (14.70 mmol) of cyclohexylisothiocyanate dissolved in 50 mL of diethyl ether. The mixture was stirred for an hour and the white solid formed was filtered off, washed with diethyl ether and vacuum dried (2.31 g, 93%). ^1H NMR ($\text{DMSO-}d_6$) δ 7.35 (1H, d, $^3J = 8.2\text{ Hz}$, NH), 4.15 (1H, m, CH), 3.86 (2H, br. s, NH_2), 2.08–1.27 (10H, m, CH_2).

2.2.3. Diacetyl-2-(4-isopropyl-3-thiosemicarbazone), HA^iPrTSC

To a suspension of 1.00 g (7.52 mmol) of $i\text{PrTSC}$ in 20 mL of water with 10 drops conc. Hydrochloric acid was added 1.5 mL (17.6 mmol) of 2,3-butanedione and the mixture was stirred for 1 h. The white solid obtained was filtered off, washed with cold water and methanol and vacuum dried (1.39 g, 92%). ^1H NMR ($\text{DMSO-}d_6$) δ 10.56 (1H, s, NH), 8.11 (1H, d, $^3J = 8.4\text{ Hz}$, NH- $i\text{Pr}$), 4.48 (1H, m, CH), 2.40 (3H, s, $\text{CH}_3\text{-CO}$), 1.95 (3H, s, $\text{CH}_3\text{-CN}$), 1.23 (6H, d, $J = 6.6\text{ Hz}$ $\text{CH}_3\text{-}i\text{Pr}$).

2.2.4. Diacetyl-2-(4-cyclohexyl-3-thiosemicarbazone), HACHTSC

The compound was obtained following the procedure described above but using 1.00 g (6.16 mmol) of ChTSC (1.31 g, 94%). ^1H NMR ($\text{DMSO-}d_6$) δ 10.59 (1H, s, NH), 8.1 (1H, d, $^3J = 8.3\text{ Hz}$, H-CH), 4.15 (1H, m, CH), 2.38 (3H, s, $\text{CH}_3\text{-CO}$), 1.95 (3H, s, $\text{CH}_3\text{-CN}$) 1.89–1.28 (10H, m, CH_2).

2.2.5. Diacetyl-2-(4-isopropyl-3-thiosemicarbazone)-3-(3-hydroxy-2-naphthohydrazide), H_2L^1

A suspension of 2.17 g (10.7 mmol) of 3-hydroxy-2-naphthohydrazide in 10.00 mL of ethanol was added to a suspension of 2.00 g (9.94 mmol) of HA^iPrTSC in 40 mL of the same solvent with eight drops of conc. hydrochloric acid. The mixture was stirred for 4 h and the cream precipitate was filtered off, washed with ethanol and vacuum dried (3.61 g, 95%). Found C: 59.02, H: 5.94, N: 18.03, S: 8.21. $\text{C}_{19}\text{H}_{23}\text{N}_5\text{O}_2\text{S}$ requires C: 59.20, H: 6.01, N: 18.17, S: 8.32. $\nu_{\text{max}}(\text{KBr})/\text{cm}^{-1}$ 3522 w (OH), 3359 m, 3342 m, 3178 m (NH), 1645 s (CO), 1628 m, 1523 s, 1496 s (thioamide II + amide II + CN), 813 w (CS). $\text{ESI}^+ m/z$ 386.10 ($[\text{M}]^+$).

2.2.6. Diacetyl-2-(4-cyclohexyl-3-thiosemicarbazone)-3-(3-hydroxy-2-naphthohydrazide), H_2L^2

To a suspension of 3.21 g (13.6 mmol) of HACHTSC in 20 mL of ethanol with six drops of conc. hydrochloric acid was added a suspension of 2.76 g (13.70 mmol) of 3-hydroxy-2-naphthohydrazide dissolved in 10 mL of ethanol. The mixture was stirred for 1 h and the cream solid was filtered off, washed with ethanol and vacuum dried (5.61 g, 94%). Found C: 62.18, H 6.37, N: 16.75, S: 7.42. $\text{C}_{22}\text{H}_{27}\text{N}_5\text{O}_2\text{S}$ requires C: 62.09, H: 6.40, N: 16.46, S: 7.53. $\nu_{\text{max}}(\text{KBr})/\text{cm}^{-1}$ 3444 sh (OH), 3352 m, 3255 m (NH), 1672s (CO), 1627 m, 1528 s (thioamide II + amide II + CN), 832 m (CS). $\text{ESI}^+ m/z$ 425.19 ($[\text{M}]^+$).

2.2.7. Diacetyl bis(3-hydroxy-2-naphthohydrazide), H_2L^3

To a suspension of 2.00 g (9.89 mmol) of 3-hydroxy-2-naphthohydrazide in 30 mL of ethanol was added 0.40 mL (4.95 mmol) of 2,3-butanedione and eight drops of conc. hydrochloric acid. The mixture was stirred during 24 h and the cream solid was filtered off, washed with ethanol and vacuum dried (2.06 g, 92%). Found C: 68.42, H 5.03, N: 11.98. $\text{C}_{26}\text{H}_{22}\text{N}_4\text{O}_4$ requires C: 68.71, H: 4.88, N: 11.96. $\nu_{\text{max}}(\text{KBr})/\text{cm}^{-1}$ 3411 w (OH), 3220 m (NH), 1649 s (CO), 1631 m (amide II + CN). $\text{ESI}^+ m/z$ 454.16 ($[\text{M}]^+$).

2.2.8. Diacetyl bis(4-cyclohexyl-3-thiosemicarbazone), H_2L^4

0.25 mL (3.10 mmol) of 2,3-butanedione was added to a suspension of 1.00 g (5.95 mmol) of ChTSC in 20 mL of ethanol with 10 drops of conc. hydrochloric acid and the mixture was refluxed for 3 h. The white precipitate was filtered off, washed with ethanol and vacuum dried (1.00 g, 85%). Found C: 54.38, H 8.33, N: 21.09, S: 15.99. $\text{C}_{18}\text{H}_{32}\text{N}_6\text{S}_2$ requires C: 54.51, H: 8.13, N: 21.19, S: 16.17. $\nu_{\text{max}}(\text{KBr})/\text{cm}^{-1}$ 3336 m, 3185 m (NH), 1525 s, 1490 s (thioamide II + CN), 867 m (CS). $\text{ESI}^+ m/z$ 396.21 ($[\text{M}]^+$).

2.2.9. $[\text{SnMe}_2\text{L}^1] \mathbf{1}$

To a boiling suspension of 100 mg (0.26 mmol) of H_2L^1 and 22 mg (0.52 mmol) of $\text{LiOH}\cdot\text{H}_2\text{O}$ in 8 mL of ethanol was added a solution of 57 mg (0.26 mmol) of SnMe_2Cl_2 in 5 mL of the same solvent. The mixture was stirred for 5 min and the resulting orange solution was immediately cooled in the fridge. After 3 h the orange precipitate formed was filtered off, washed with cold ethanol and vacuum dried (110 mg, 80%). Found C: 47.22, H: 4.93, N: 13.06, S: 5.90. $\text{SnC}_{21}\text{H}_{27}\text{N}_5\text{O}_2\text{S}$ requires C: 47.39, H: 5.11, N: 13.16, S: 6.02. $\nu_{\text{max}}(\text{KBr})/\text{cm}^{-1}$ 3431 s (OH), 3266 m (NH), 1642 m (CO), 1530 m (thioamide II + amide II + CN), 821 w (CS). $\text{ESI}^+ m/z$ 534.09 ($[\text{M} + \text{H}]^+$).

2.2.10. $[\text{SnBu}_2\text{L}^1] \mathbf{2}$

This complex was obtained following the same procedure described for the synthesis of **1** but adding 79 mg (0.26 mmol) of SnBu_2Cl_2 (red, 141 mg, 88%). Slow evaporation of a solution in DMF yielded crystals suitable for single crystal X-ray diffraction. Found C: 52.36, H: 6.28, N: 11.19, S: 5.12. $\text{SnC}_{27}\text{H}_{39}\text{N}_5\text{O}_2\text{S}$ requires C: 52.58, H: 6.38, N: 11.36, S: 5.20. $\nu_{\text{max}}(\text{KBr})/\text{cm}^{-1}$ 3437 m (OH), 3266 m (NH), 1641 m (CO), 1536 s (thioamide II + amide II + CN), 808 w (CS). $\text{ESI}^+ m/z$ 618.19 ($[\text{M} + \text{H}]^+$).

2.2.11. $[\text{SnPh}_2\text{L}^1(\text{OH}_2)] \mathbf{3}$

This complex was obtained following the same procedure described for the synthesis of **1** but adding 89 mg (0.26 mmol) of SnPh_2Cl_2 (dark orange, 148 mg, 87%). Slow evaporation of a solution in DMF yielded crystals suitable for single crystal X-ray diffraction. Found C: 55.39, H: 4.96, N: 10.49, S: 4.69. $\text{SnC}_{31}\text{H}_{33}\text{N}_5\text{O}_3\text{S}$ requires C: 55.21, H: 4.93, N: 10.38, S: 4.75. $\nu_{\text{max}}(\text{KBr})/\text{cm}^{-1}$ 3437 m (OH), 3266 m (NH), 1641 m (CO), 1536s (thioamide II + amide II + CN), 808 w (CS). $\text{ESI}^+ m/z$ 618.19 ($[\text{M}-\text{OH}_2 + \text{H}]^+$).

2.2.12. $[\text{SnMe}_2\text{L}^2] \mathbf{4}$

To a suspension of 100 mg (0.24 mmol) of H_2L^2 and two equivalents of $\text{LiOH}\cdot\text{H}_2\text{O}$ in 10 mL of ethanol was added 52 mg (0.24 mmol) of SnMe_2Cl_2 dissolved in 5 mL of the same solvent and the mixture was refluxed for 3 h. The red solid formed was filtered off, washed with cold ethanol and vacuum dried (98 mg, 70%). Slow evaporation of a solution in acetone yielded crystals suitable for single crystal X-ray diffraction. Found C: 50.20, H: 5.35, N: 12.07, S: 5.42. $\text{SnC}_{24}\text{H}_{31}\text{N}_5\text{O}_2\text{S}$ requires C: 50.38, H: 5.46, N: 12.24, S: 5.59. $\nu_{\text{max}}(\text{KBr})/\text{cm}^{-1}$ 3430 w (OH), 3370 m (NH), 1640 m (CO), 1579 m, 1535 m (thioamide II + amide II + CN), 811 w (CS). $\text{ESI}^+ m/z$ 574.13 ($[\text{M} + \text{H}]^+$).

2.2.13. $[\text{SnBu}_2\text{L}^2] \mathbf{5}$

To a suspension of 100 mg (0.24 mmol) of H_2L^2 and two equivalents of $\text{LiOH}\cdot\text{H}_2\text{O}$ in 10 mL of ethanol was added 71 mg (0.24 mmol) of SnBu_2Cl_2 dissolved in 8 mL of the same solvent and the mixture was refluxed for 3 h. The red solution obtained was concentrated until a red solid appeared, that was filtered off and vacuum dried (red, 120 mg, 81%). Slow evaporation of a solution in acetone yielded crystals suitable for single crystal X-ray diffraction. Found C: 54.72, H: 6.48, N: 10.50, S: 4.79. $\text{SnC}_{30}\text{H}_{43}\text{N}_5\text{O}_2\text{S}$ requires C: 54.89, H: 6.60, N: 10.67, S: 4.88. $\nu_{\text{max}}(\text{KBr})/\text{cm}^{-1}$ 3430 w (OH), 3309 m (NH), 1641 m (CO), 1577 m, 1533 s (thioamide II + amide II + CN), 835 w (CS). $\text{ESI}^+ m/z$ 658.22 ($[\text{M} + \text{H}]^+$).

2.2.14. $[\text{SnPh}_2\text{L}^2(\text{OH}_2)] \mathbf{6}$

This complex was obtained following the same procedure described for the synthesis of **4**, but adding 84 mg (0.24 mmol) of SnPh_2Cl_2 (orange, 155 mg, 92%). Found C: 58.59, H: 5.04, N: 9.89, S: 4.44. $\text{SnC}_{34}\text{H}_{35}\text{N}_5\text{O}_2\text{S}$ requires C: 58.64, H: 5.07, N: 10.06, S: 4.60. $\nu_{\text{max}}(\text{KBr})/\text{cm}^{-1}$ 3430 w (OH), 3392 m (NH), 1639 m (CO), 1573 m, 1523 s (thioamide II + amide II + CN), 833 w (CS). $\text{ESI}^+ m/z$ 698.16 ($[\text{M}-\text{OH}_2 + \text{H}]^+$).

2.2.15. $[\text{SnMe}_2\text{L}^3] \mathbf{7}$

To a suspension of 100 mg (0.22 mmol) of H_2L^3 and 18 mg (0.44 mmol) of $\text{LiOH}\cdot\text{H}_2\text{O}$ in 12 mL of ethanol was added 48 mg (0.22 mmol) of SnMe_2Cl_2 dissolved in 5 mL of the same solvent and the mixture was stirred for 24 h. The bright yellow solid formed was filtered off, washed with cold ethanol and vacuum dried (119 mg, 90%). Slow evaporation of a solution in DMF afforded crystals suitable for single crystal X-ray diffraction. Found C: 55.81, H: 4.51, N: 9.16. $\text{SnC}_{28}\text{H}_{26}\text{N}_4\text{O}_4$ requires C: 55.93, H: 4.36, N: 9.32. $\nu_{\text{max}}(\text{KBr})/\text{cm}^{-1}$ 3430 s (OH + NH), 1639 m (CO), 1610 w (CN). $\text{ESI}^+ m/z$ 603.11 ($[\text{M} + \text{H}]^+$).

2.2.16. $[\text{SnBu}_2\text{L}^3] \mathbf{8}$

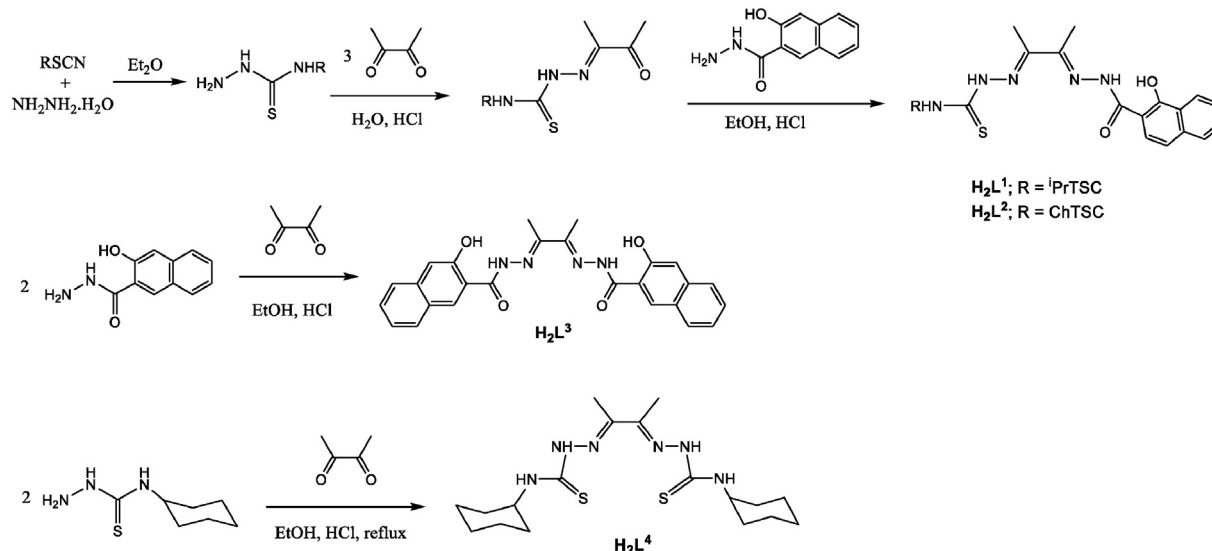
This complex was obtained following the same procedure described for the synthesis of **7**, but adding 67 mg (0.22 mmol) of SnBu_2Cl_2 to yield an orange solid (129 mg, 86%). Found C: 59.43, H: 5.51, N: 8.05. $\text{SnC}_{34}\text{H}_{38}\text{N}_4\text{O}_4$ requires C: 59.58, H: 5.59, N: 8.17. $\nu_{\text{max}}(\text{KBr})/\text{cm}^{-1}$ 3433 m (OH + NH), 1641 m (CO), 1606 w (CN). $\text{ESI}^+ m/z$ 687.20 ($[\text{M} + \text{H}]^+$).

2.2.17. $[\text{SnPh}_2\text{L}^3(\text{EtOH})] \mathbf{9}$

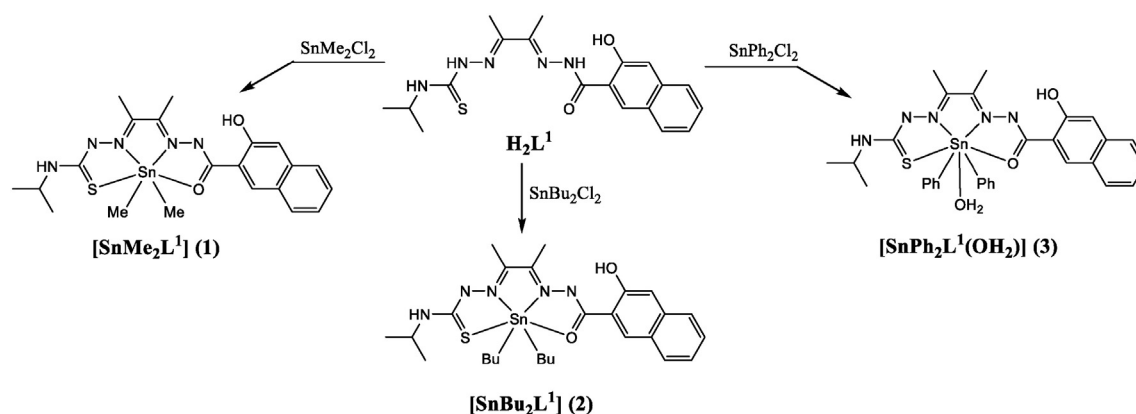
This complex was obtained following the same procedure described for the synthesis of **7**, but adding 76 mg (0.22 mmol) of SnPh_2Cl_2 to yield a pale orange solid (139 mg, 88%). Slow evaporation of a solution in DMSO yielded crystals suitable for single crystal X-ray diffraction. Found C: 62.05, H: 4.85, N: 7.11. $\text{SnC}_{40}\text{H}_{36}\text{N}_4\text{O}_5$ requires C: 62.28, H: 4.70, N: 7.26. $\nu_{\text{max}}(\text{KBr})/\text{cm}^{-1}$ 3434 s (OH + NH), 1643 m (CO), 1607 w (CN). $\text{ESI}^+ m/z$ 727.14 ($[\text{M}-\text{EtOH} + \text{H}]^+$).

2.2.18. $[\text{Sn}(\text{L}^2)_2] \mathbf{10}$

To a suspension of 100 mg (0.24 mmol) of H_2L^2 and two equivalents of $\text{LiOH}\cdot\text{H}_2\text{O}$ in 10 mL of ethanol was added 147 mg (0.24 mmol) of SnI_4 dissolved in 4 mL of ethanol and the mixture was refluxed for 2 h. The orange solid was filtered off, washed with cold ethanol and vacuum dried (164 mg, 72%). Slow evaporation of the mother liquor yielded crystals suitable for single crystal X-ray diffraction. Found C: 54.81, H: 5.16, N: 14.66, S: 6.51. $\text{SnC}_{44}\text{H}_{50}\text{N}_{10}\text{O}_4\text{S}_2$ requires C: 54.72, H: 5.22, N: 14.50, S: 6.64. $\nu_{\text{max}}(\text{KBr})/\text{cm}^{-1}$ 3413 m (OH), 3372 m (NH), 1641 m (CO), 1573w, 1535 m (thioamide II + amide II + CN), 829 w (CS). $\text{ESI}^+ m/z$ 927.27 ($[\text{M} + \text{H}]^+$).



Scheme 1. Synthesis of the ligands.



Scheme 2. Structures of the complexes obtained from H_2L^1 and 2 equiv. of $LiOH \cdot H_2O$.

2.2.19. $[SnI_2L^2]$ **11**

To a suspension of 100 mg (0.24 mmol) of H_2L^2 in 10 mL of ethanol was added 147 mg (0.24 mmol) of SnI_4 dissolved in 4 mL of ethanol and the mixture was stirred for 2 h. The yellow solid was filtered off, washed with cold ethanol and vacuum dried (154 mg, 82%). $\Lambda_M(\Omega^{-1} \text{ cm}^2 \text{ mol}^{-1})$ 123.3 (in DMF) and 23.9 (in acetone). Found C: 33.12, H: 3.11, N: 8.97, S: 3.89. $SnC_{22}H_{25}N_5SO_2I_2$ requires C: 33.19, H: 3.17, N: 8.80, S: 4.03. $\nu_{\max}(\text{KBr})/\text{cm}^{-1}$ 3479 m (OH), 3264 m (NH), 1637 m (CO), 1571 s, 1515 m (thioamide II + amide II + CN), 821 w (CS). $ESI^+ m/z$ 669.00 $[M - I]^+$.

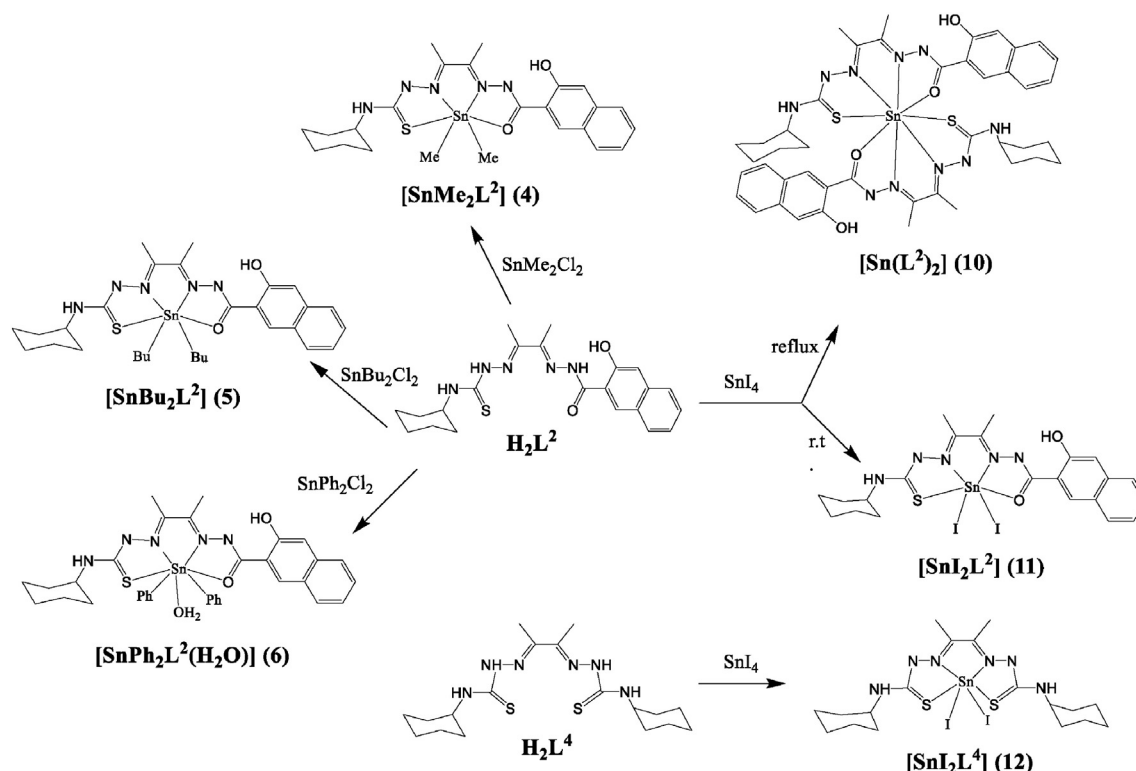
2.2.20. $[SnI_2L^4]$ **12**

To a suspension of 100 mg (0.25 mmol) of H_2L^4 in 10 mL of ethanol with two equivalents of $LiOH \cdot H_2O$ was added 158 mg (0.25 mmol) of SnI_4 dissolved in 4 mL of ethanol and the mixture was refluxed for 3 h. The red solid was filtered off, washed with cold ethanol and vacuum

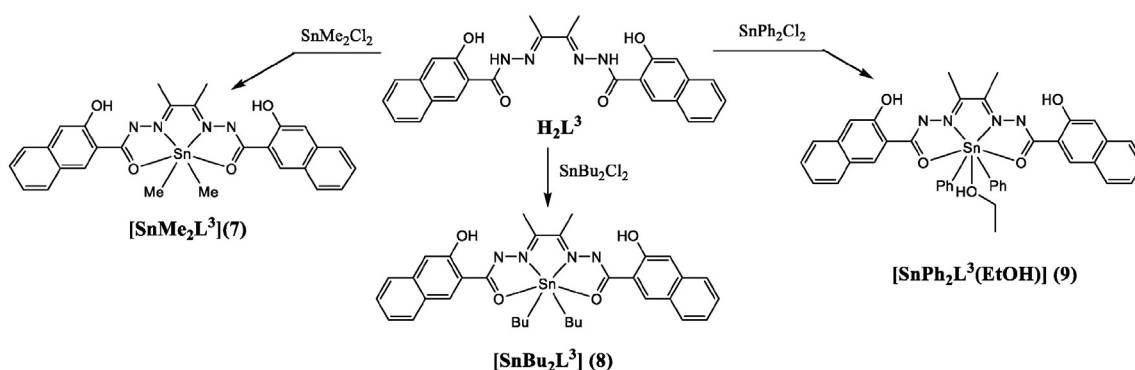
dried (167 mg, 87%). $\Lambda_M(\Omega^{-1} \text{ cm}^2 \text{ mol}^{-1})$ 66.0 (in DMF) and 13.3 (in acetone) Found C: 28.35, H: 3.95, N: 10.88, S: 8.20. $SnC_{18}H_{30}N_6S_2I_2$ requires C: 28.18, H: 3.94, N: 10.96, S: 8.36. $\nu_{\max}(\text{KBr})/\text{cm}^{-1}$ 3265 m (NH), 1502 s, 1475 s (thioamide II + amide II + CN), 813 w (CS). $ESI^+ m/z$ 641.00 $[M - I]^+$.

2.3. X-ray crystallography

Data were acquired using a Bruker AXS Kappa Apex-II diffractometer equipped with an Apex-II CCD area detector using a graphite monochromator (Mo K_α radiation, $\lambda = 0.71073 \text{ \AA}$). The substantial redundancy in data allows empirical absorption corrections (SADABS) [33] to be applied using multiple measurements of symmetry-equivalent reflections. The raw intensity data frames were integrated with the SAINT program, which also applied corrections for Lorentz and polarization effects [34].



Scheme 3. Structures of the complexes obtained from H_2L^2 and H_2L^4 . All the complexes were obtained in the presence of $LiOH \cdot H_2O$ but **11**.



Scheme 4. Structures of the complexes obtained from H_2L^3 and 2 equiv. of $\text{LiOH} \cdot \text{H}_2\text{O}$.

The software package SHELXTL version 6.10 was used for space group determination, structure solution and refinement. The structures were solved by direct methods (SHELXS-97) [35], completed with difference Fourier syntheses, and refined with full-matrix least squares using SHELXL-97 minimizing $\omega(F_o^2 - F_c^2)$. Weighted R factors (R_w) and all goodness of fit S are based on F^2 ; conventional R factors (R) are based on F [36]. All non-hydrogen atoms were refined with anisotropic displacement parameters. The hydrogen atoms were located in a difference Fourier map and their coordinates and isotropic thermal parameters subsequently refined, except H2 in complexes 5 and 10. EtOH that were positioned geometrically after each cycle of refinement. All scattering factors and anomalous dispersion factors are contained in the SHELXTL 6.10 program library. Due to the disorder found in the DMF of recrystallization of complex 2, the hydrogen atoms or the methyl groups are omitted from the model, but they are included in calculations of the formula weight etc.

CCDC 1458713–9 for complexes 2.0.5DMF, 3, 4, 5, 7.DMF, 9 and 10.EtOH respectively contain the supplementary crystallographic data for this paper. These data can be obtained free of charge from the Cambridge Crystallographic Data Centre via www.ccdc.cam.ac.uk/data_request/cif.

2.4. Antimicrobial activity

The *in vitro* antimicrobial properties of the designed ligands, their corresponding complexes and parent organotin(IV) compounds were studied by determining their minimum inhibitory concentrations (MICs) by means of the broth two-fold dilution procedure [37]. The antibacterial activity was detected against Gram positive (*Bacillus subtilis* ATCC 6633, *Staphylococcus aureus* ATCC 25923) and Gram negative (*Escherichia coli* ATCC 8739, *Haemophilus influenzae* ATCC 19418) bacteria. For the antifungal bioassay, yeasts (*Candida tropicalis* ATCC 1369, *Saccharomyces cerevisiae* ATCC 9763) and mould (*Aspergillus niger* ATCC 6275) were used as test microorganisms.

Compounds were dissolved in dimethyl sulfoxide and diluted in the media (*Haemophilus* test medium for *Haemophilus influenzae*, Mueller Hinton broth for the other bacteria, Sabouraud liquid medium for fungi) (Oxoid, Basingstoke, UK) to final concentrations ranging from 200 to $0.0015 \mu\text{g mL}^{-1}$. In all cases, DMSO never exceeded the amount of 1% v/v and control tubes for solvent were also maintained in each experiment. Aliquots of the bacterial and fungal suspensions were mixed with the chemicals to obtain an inoculum size of $5 \cdot 10^5$ colony forming units/mL and $5 \cdot 10^3$ cells/mL, respectively. Bacteria were then incubated

Table 1

Crystal data and structure refinement for compounds [2DMF]0.5DMF, [3DMF], [4H₂O], 5, [7DMF].DMF, [9DMSO] and 10.EtOH.

Formula	[2DMF]0.5DMF	[3DMF]	[4H ₂ O]	5	[7DMF].DMF	[9DMSO]	10.EtOH
Formula	SnC _{31.5} H _{49.50} N _{6.50} O _{3.50} S	SnC ₃₄ H ₃₈ N ₆ O ₃ S	SnC ₂₄ H ₃₃ N ₅ O ₃ S	SnC ₃₀ H ₄₃ N ₅ O ₂ S	SnC ₃₄ H ₄₀ N ₆ O ₆	SnC ₄₀ H ₃₆ N ₄ O ₅ S	SnC ₄₆ H ₅₆ N ₁₀ O ₅ S
M	726.03	729.45	590.30	656.44	747.41	803.48	1011.82
Temperature/K	100(2)	296(2)	296(2)	296(2)	296(2)	296(2)	296 (2)
Crystal system	Triclinic	Monoclinic	Monoclinic	Triclinic	Triclinic	Triclinic	Monoclinic
Space group	P-1	P2(1)/c	P2(1)/c	P-1	P-1	P-1	C2/c
a/Å	10.9072(9)	10.2681(2)	12.4969(8)	8.4620(3)	11.4637(4)	8.8160(3)	13.467(2)
b/Å	12.0929(8)	32.8041(6)	11.8037(8)	14.4046(5)	12.3852(4)	12.1950(5)	35.042(6)
c/Å	14.7622(12)	10.6313(2)	17.0615(12)	14.5715(4)	14.5293(6)	17.4115(6)	13.346(2)
$\alpha/^\circ$	94.428(3)	90	90	106.2320(10)	86.392(2)	80.067(2)	90
$\beta/^\circ$	105.560(4)	106.5480(10)	94.513(2)	98.450(2)	69.502(2)	88.213(2)	119.406(8)
$\gamma/^\circ$	108.296(3)	90	90	103.385(2)	64.145(2)	71.934(2)	90
U/Å ³	1753.0(2)	1.411	2508.9(3)	1615.87(9)	1728.93(11)	1752.47(11)	1113(4)
Z	2	4	4	2	2	2	4
D _c /Mgm ⁻³	1.375	1.411	1.563	1.349	1.436	1.523	1.225
Absorption coefficient mm ⁻¹	0.830	0.847	1.137	0.888	0.791	0.841	0.590
F(000)	756	1496	1208	680	768	820	2096
Goodness of fit on F ²	1.232	1.175	1.063	1.091	1.250	1.147	1.148
Reflections collected	57,958	58,423	51,351	67,408	92,182	57,052	43,415
Independent reflections	6407 [R(int) = 0.0353]	6261 [R(int) = 0.0309]	6225 [R(int) = 0.0442]	8033 [R(int) = 0.0305]	6296 [R(int) = 0.0377]	5757 [R(int) = 0.0450]	5588 [R(int) = 0.0599]
Final R1 and wR2 [I > 2 σ (I)]	0.0228, 0.0682	0.0373, 0.1032	0.0252, 0.0659	0.0379, 0.0996	0.0289, 0.0783	0.0294, 0.0722	0.0622, 0.2070
R indices (all data)	R1 = 0.0293, wR2 = 0.0836	R1 = 0.0452, wR2 = 0.1170	R1 = 0.0361, wR2 = 0.0830	R1 = 0.0573, wR2 = 0.1210	R1 = 0.0376, wR2 = 0.0991	R1 = 0.0409, wR2 = 0.0852	R1 = 0.0990, wR2 = 0.2370
Residual electron density (min,max) (eÅ ⁻³)	−0.412, 0.537	−0.620, 0.950	−0.651, 0.665	−0.678, 0.612	−0.416, 0.438	−0.700, 0.729	−0.689, 1.911

Table 2Selected bond distances (Å) and angles (°) in complexes [2DMF]0.0.5DMF, [3DMF], [4H₂O], 5 and 10.EtOH.

	[2DMF]0.0.5DMF	[3DMF]	[4H ₂ O]	5	10.EtOH
Sn(1)–C(20)/C(23)	2.137(2)	2.162(4)	2.123(2)	2.133(4)	–
Sn(1)–C(26)/C(24)/C(27)	2.141(2)	2.163(4)	2.117(2)	2.134(4)	–
Sn(1)–O(1)	2.3128(17)	2.312(2)	2.4069(15)	2.373(2)	2.150(4)
Sn(1)–N(3)	2.370(2)	2.345(3)	2.3546(19)	2.280(2)	2.399(5)
Sn(1)–N(4)	2.309(2)	2.326(3)	2.3140(19)	2.242(2)	2.297(5)
Sn(1)–S(1)	2.7098(7)	2.5996(11)	2.6583(6)	2.6970(9)	2.5245(18)
Sn(1)–O(3)	2.5080(17)	2.383(3)	2.4569(17)	–	–
C–Sn–C	171.11(10)	170.32(14)	168.90(10)	152.54(18)	–

Table 3

Selected bond distances (Å) and angles (°) in complexes [7DMF].DMF and [9DMSO].

	[7DMF].DMF	[9DMSO]
Sn(1)–C(27)	2.115(3)	2.132(2)
Sn(1)–C(28)/C(33)	2.111(3)	2.144(2)
Sn(1)–O(1)	2.254(2)	2.2250(15)
Sn(1)–O(3)	2.331(4)	2.2478(15)
Sn(1)–N(3)	2.346(2)	2.3259(18)
Sn(1)–N(4)	2.327(2)	2.3140(19)
Sn(1)–O(5)	2.372(2)	2.3064(18)
C–Sn–C	172.42(14)	175.10(8)

at 37 °C for 24 h and fungi at 30 °C for 48 h. Ampicillin and miconazole were tested under identical conditions as antibacterial and antifungal reference drugs, respectively. The minimum inhibitory concentrations (MIC, µg mL^{−1}) were recorded as the lowest concentration of compound that inhibits visible growth of the tested microorganisms.

The minimum bactericidal concentrations (MBCs) and the minimum fungicidal concentrations (MFCs) were determined by subculturing on fresh sterile medium 100 µL of culture from each sample remained clear. MBC and MFC values represented the lowest concentration of compound (µg mL^{−1}) showing 99% inhibition after incubation period of bacteria at 37 °C for 24 h and of fungi at 30 °C for 48 h.

Each experiment was performed in triplicate and repeated at least three times.

Results and discussion

2.5. Synthesis

Two new mixed thiosemicarbazone/hydrazone ligands **H₂L¹** and **H₂L²** were synthesized by reaction of 3-hydroxy-2-naphthohydrazide

with diacetyl-2-(4-isopropyl-3-thiosemicarbazone) or diacetyl-2-(4-cyclohexyl-3-thiosemicarbazone) respectively. Moreover, the symmetric molecules diacetyl bis(3-hydroxy-2-naphthohydrazide) and diacetyl bis(4-cyclohexyl-3-thiosemicarbazone), **H₂L³** and **H₂L⁴** respectively, were also obtained reacting 2,3-butanedione with two equivalents of the hydrazine or cyclohexyl-thiosemicarbazide (Scheme 1).

The synthesis of the monothiosemicarbazones was achieved with a substantial modification of the procedure reported in the literature for analogous compounds [38], in which the reaction must be carried out in water at 0 °C with an exhaustive control of the temperature and which always led to the formation of a small amount of the bis(thiosemicarbazone). The procedure reported in this paper completely prevents the formation of undesired products and is easier, since it is at room temperature.

Reactions of the dissymmetric ligands **H₂L¹** and **H₂L²** and the bis(hydrazone) **H₂L³** with the organotin(IV) derivatives SnR₂Cl₂ (X = Me, *n*-Bu, Ph) were carried out in ethanol and in the presence of two equivalents of lithium hydroxide to induce ligand deprotonation. Pure complexes **1–9** (Schemes 2, 3 and 4) were obtained in good yield with the reaction conditions described in the experimental part. It is worth noting the differences in the reactivity of both dissymmetric ligands: while **H₂L²** leads to the same complexes under all the reaction conditions studied, **H₂L¹** rapidly evolves to the bis(hydrazone) and complexes with this ligand were formed under most of the conditions studied. To prevent this symmetrization, the reaction time was reduced to only 5 min and the mixture was rapidly cooled in the fridge, conditions that led to formation of the pure complexes **1–3**.

Reactions of **H₂L²** and **H₂L⁴** with tin(IV) iodide were carried out both in the presence and in the absence of LiOH·H₂O and at different temperatures. Reactions of **H₂L²** only depend on the presence or the absence of basic medium, leading to the isolation of complexes **10** and **11**

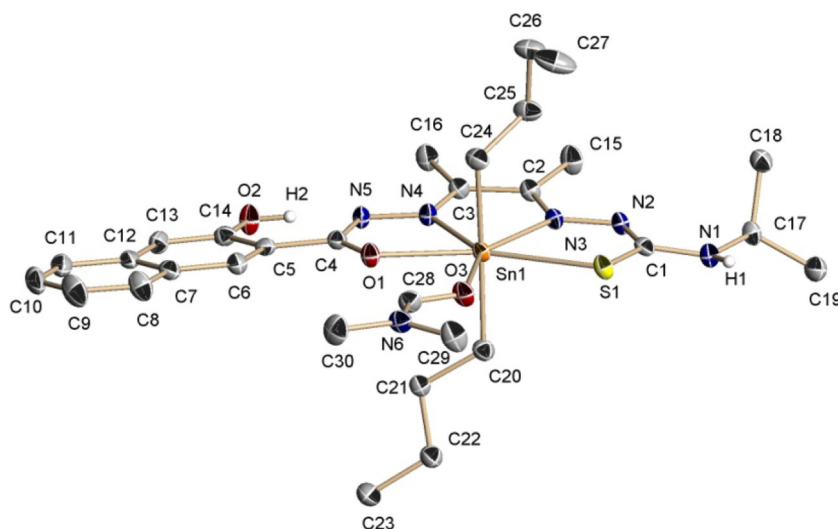


Fig. 1. Molecular structure of complex [SnBu₂(DMF)L¹], [2DMF]0.0.5DMF. Thermal ellipsoids at 50% probability level. The hydrogen atoms, except H1 and H2, and the DMF molecule of recrystallization are omitted for clarity.

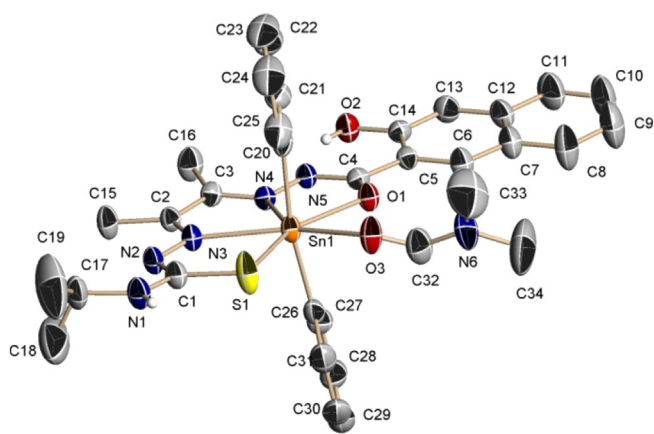


Fig. 2. Molecular structure of complex $[\text{SnPh}_2(\text{DMF})\text{L}^1]$, $[\text{3DMF}]$. Thermal ellipsoids at 40% probability level. The hydrogen atoms, except H1 and H2, are omitted for clarity.

(Scheme 3). However, complex **12**, analogous to complex **11** but containing H_2L^4 (Scheme 3), was exclusively obtained in the presence of $\text{LiOH} \cdot \text{H}_2\text{O}$ under reflux and with any other reaction conditions mixtures that could not be characterized were obtained.

The analytical data of all the complexes show the dianionic behavior of the ligand and, except for complex **10**, confirm a 1:1 ligand to metal ratio, while for complex **10** agree with a 1:2 Sn:L stoichiometry. For complexes **1–9** also indicate the presence of the corresponding organic groups bonded to the tin atom. On other hand, for complexes **11** and **12** show the presence of two iodide ions. The mass spectra of complexes **1–9** only show the peak corresponding to $[\text{SnR}_2\text{L} + \text{H}]^+$, confirming the proposed stoichiometry. Mass spectrum of complex **10** shows a peak corresponding to $[\text{M} + \text{H}]^+$, while the mass spectra of complexes **11** and **12** display a peak corresponding to the loss of one of the iodide ligands. For all the peaks the found and calculated isotopic patterns are identical.

Molar conductivity in acetone for complex **11** ($23.9 \Omega^{-1} \text{cm}^2 \text{mol}^{-1}$) corresponds to a molecular species showing that both iodides are bonded to the metal, while in DMF ($123.3 \Omega^{-1} \text{cm}^2 \text{mol}^{-1}$) is close to the value expected for 1:2 electrolytes suggesting the solvolysis of I^- by DMF molecules [39]. A similar behavior is observed for complex **12**, which in

acetone behaves as a molecular species ($13.3 \Omega^{-1} \text{cm}^2 \text{mol}^{-1}$), but in DMF as a 1:1 electrolyte ($66.0 \Omega^{-1} \text{cm}^2 \text{mol}^{-1}$).

2.6. Crystal structures

The molecular structure of seven compounds could be determined by single crystal X-ray diffraction. The crystallographic and refinement data are collected in Table 1 and selected bond distances are listed in Tables 2 and 3. In all the complexes the ligand is doubly deprotonated and behaves as a tetradentate donor (N_2O_2 in complexes $[\text{2DMF}]\text{0.5DMF}$, $[\text{3DMF}]$, $[\text{4H}_2\text{O}]$, **5** and **10**. EtOH and N_2O_2 in complexes $[\text{7DMF}]\text{DMF}$ and $[\text{9DMSO}]$), coordination mode that confers high stability due to the formation of three five-member chelate rings. The double deprotonation induces a great deal of electronic delocalization in the ligand skeleton and therefore bond distances are intermediate between single and double bonds. In all the complexes there is an intramolecular hydrogen bond between the OH group and the deprotonated hydrazinic nitrogen. The C—Sn—C bond angles, except for complex **5**, range from 168.90 to 175.10° and are close to the expected value (180°) for both octahedral and pentagonal bipyramid arrangements in which the organic groups are axially coordinated. In complex **5** this value is significantly lower (152.54°), probably due to steric requirements.

When the complexes are recrystallized in DMF or DMSO, a molecule of the corresponding solvent is bonded to the tin atom, leading to an increase of the coordination number or to a substitution of a water or ethanol molecule.

The crystal structure of complex **2** contains discrete molecules of $[\text{SnBu}_2(\text{DMF})\text{L}^1]$ and half a molecule of DMF delocalized over two positions. In the complex the tin atom is hepta-coordinated to two butyl groups, one ligand and one DMF molecule in a distorted pentagonal bipyramid environment with the organic groups in the axial positions (Fig. 1). The DMF molecule has occupied a vacant position and increased the coordination number from six to seven. The ligand is slightly buckled, with a maximum deviation from the least-square plane of 0.102 \AA for S1 and the angle with the naphthol ring is 10.44° . The butyl groups have different conformation, while one of them is *anti* the other is *gauche*, probably due to steric requirements. A similar conformation was previously observed in other complexes with related ligands [40].

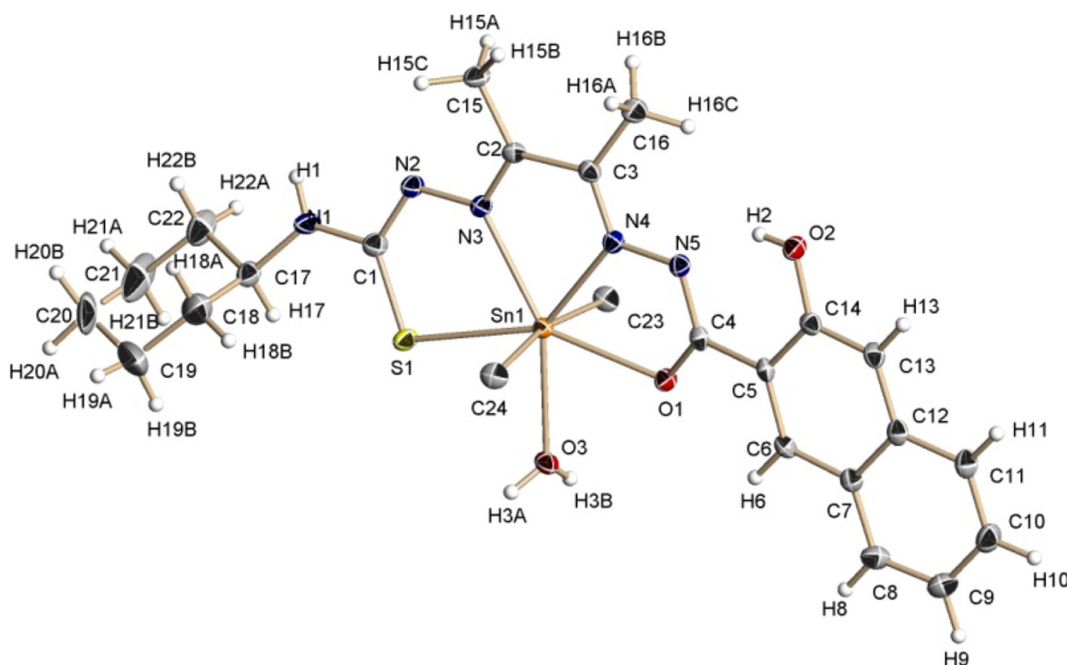


Fig. 3. Molecular structure of complex $[\text{SnMe}_2\text{L}^2(\text{OH}_2)]$, $[\text{4H}_2\text{O}]$. Thermal ellipsoids at 50% probability level.

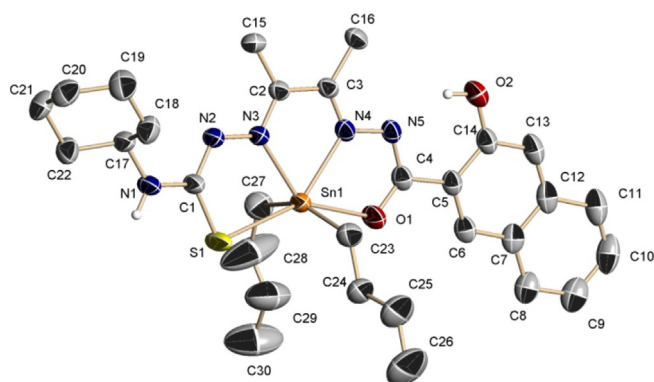


Fig. 4. Molecular structure of complex $[\text{SnBu}_2\text{L}^2]$, **5**. Thermal ellipsoids at 30% probability level. The hydrogen atoms, except H1 and H2, are omitted for clarity.

When complex **3** is recrystallized in DMF, the water molecule present is replaced by DMF, so the tin atom is hepta-coordinated to two phenyl groups, one ligand and one DMF molecule in a distorted pentagonal bipyramid environment with the organic groups in the axial positions (Fig. 2) in an analogous environment to that of complex **2**. The ligand

core is more planar, with a maximum deviation from the least-square plane of 0.076 Å for C3 and with the naphthol ring almost coplanar. The phenyl rings are almost perpendicular to the ligand skeleton and are coplanar, with a rotation angle between them of 4.62°.

The molecular structure of complex **4** is similar to that of complexes **2** and **3**, but with methyl groups and H_2O bonded to the metal (Fig. 3). The ligand is considerably less planar with maximum deviation from the least-square plane of 0.187 Å for O1 but the dihedral angle between the naphthol and the ligand core is 4.54°. Both hydrogen of the water molecule are involved in hydrogen bonds with N2 and O1, leading to the formation of infinite sheets in the *bc* plane.

The crystal structure of complex **5** consists of $[\text{SnBu}_2\text{L}^2]$ units in which the tin atom is hexa-coordinated to one ligand and two butyl groups in the apical positions of a distorted octahedron (Fig. 4). The maximum deviation from the least-square plane of the ligand core is 0.1144 Å for O1 and its dihedral angle with the naphthol is 9.28°. In this complex both butyl groups are in anti disposition.

The molecular structure of complex **7** shows $[\text{SnMe}_2(\text{DMF})\text{L}^3]$ units and a DMF molecule of crystallization (Fig. 5). As occurs in complex **2**, the DMF molecule has occupied a vacant position and increased the coordination number from six to seven, so the tin atom is bonded to one ligand, one DMF molecule and two methyl groups axially coordinated

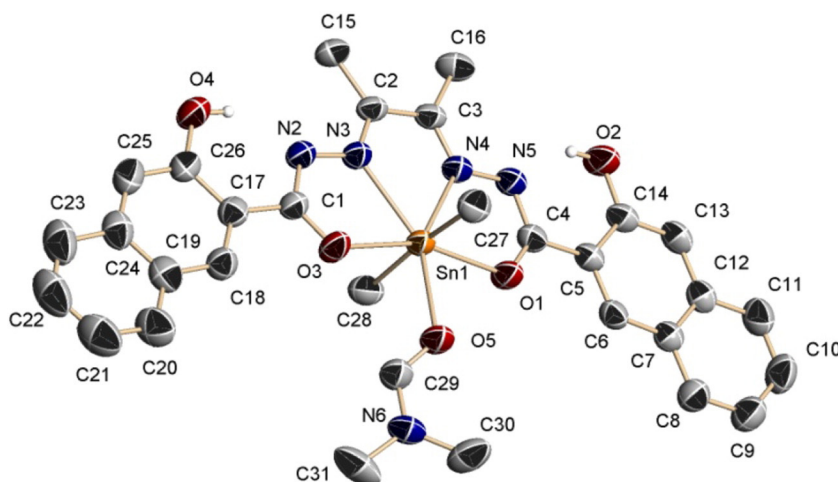


Fig. 5. Molecular structure of complex $[\text{SnMe}_2(\text{DMF})\text{L}^3]$, **[7DMF].DMF**. Thermal ellipsoids at 50% probability level. The hydrogen atoms, except H2 and H4, and the DMF molecule of recrystallization are omitted for clarity.

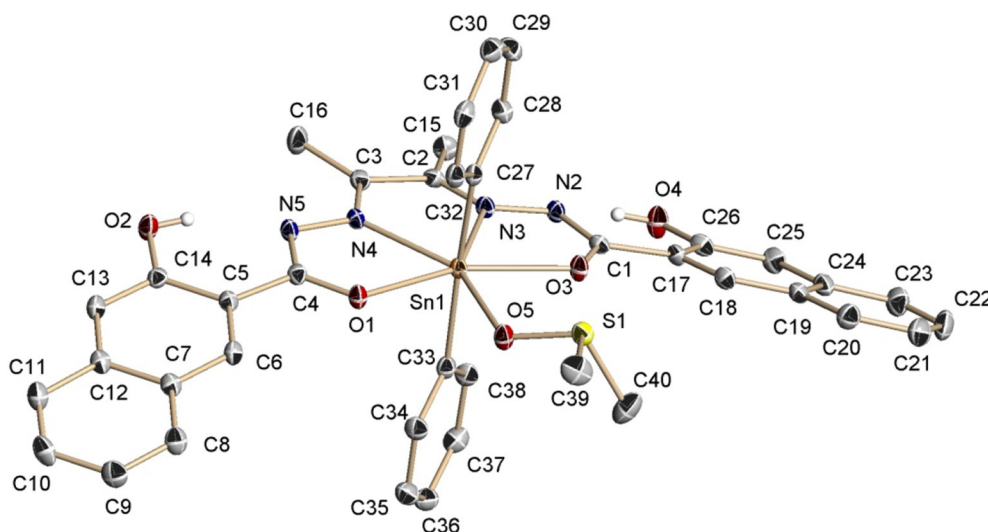


Fig. 6. Molecular structure of complex $[\text{SnPh}_2(\text{DMSO})\text{L}^3]$, **[9DMSO]**. Thermal ellipsoids at 50% probability level. The hydrogen atoms, except H2 and H4, are omitted for clarity.

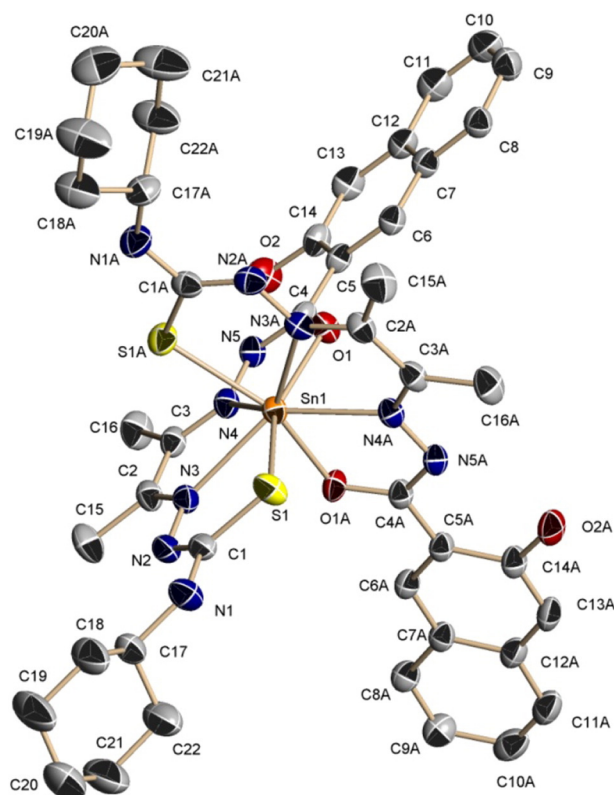


Fig. 7. Molecular structure of complex $[\text{Sn}(\text{L}^2)_2] \cdot 10\text{EtOH}$. Thermal ellipsoids at 30% probability level. The hydrogen atoms and the EtOH molecule of recrystallization are omitted for clarity.

in a pentagonal bipyramid arrangement. The analogous situation is observed in the crystal structure of complex **9**, in which the ethanol molecule has been replaced by DMSO (Fig. 6). In both complexes the bis(hydrazone) core is deviated from planarity, with a maximum deviation of O3 from the least-square plane of 0.1433 Å for complex **7** and 0.1345 Å for complex **9**. The main difference between both complexes is that in complex **7** one of the naphthol rings is coplanar with the bis(hydrazone) core and the other forms an angle of 12.03°, while in complex **9** the ligand is considerably buckled with a dihedral angle between the naphthol groups of 37.42°, since none of the naphthol groups are coplanar with the ligand core. In complex **9** there is a π - π stacking between the rings formed by C5–C6–C7–C12–C13–C14, with a distance between centroids of 3.938 Å, leading to the formation of dimers (Fig. S1), while in complex **7** the presence of a DMF molecule of crystallization prevents this stacking.

Complex **10** crystallizes with a molecule of ethanol and its crystal packing is made up by $[\text{Sn}(\text{L}^2)_2]$ units in which the tin atom is

coordinated to two ligands in a $\text{N}_4\text{O}_2\text{S}_2$ environment with a distorted dodecahedral arrangement (Fig. 7). The ligand core is virtually planar with maximum deviation from the least-square plane of 0.048 Å for C2 and with a dihedral angle between the naphthol and the ligand of 2.9°. The naphthol groups are stacked by double π - π interactions with a distance between centroids of 3.707 Å leading to the formation of infinite chains along the *a* axis (Fig. S2).

2.7. IR spectroscopy

The IR spectra of the organic molecules show the bands corresponding to the expected functional groups (*vide infra*), and therefore they confirm the formation of the two new dissymmetric thiosemicarbazone ligands (H_2L^1 and H_2L^2), and the two symmetric ones bis(3-hydroxy-2-naphthohydrazone) and bis(4-cyclohexyl-3-thiosemicarbazone), H_2L^3 and H_2L^4 respectively. In the IR spectra of the complexes, the number of bands corresponding to the $\nu(\text{NH})$ vibrations decreases indicating the deprotonation of the ligands. The shifts observed in the bands assigned to $\nu(\text{CN})$, $\nu(\text{CS})$ and $\nu(\text{CO})$ are consistent with the imine, thiocarbonyl and carbonyl groups are bonded to the tin atom in all the complexes confirming that the ligands behave as N_2OS , N_2O_2 or N_2S_2 donors. Moreover, spectra of **3**, **6** and **9** show additional bands corresponding to the water or ethanol molecules coordinated to the metal.

2.8. NMR spectroscopy

The atom labelling used in the NMR assignments is shown in Fig. 8. The ^1H NMR spectra of all the organic molecules display chemical shifts, intensities and multiplicities consistent with the proposed structures. The ^1H NMR spectra of all the complexes (Table 4) confirm that the ligands are doubly deprotonated, due to the loss of the signal corresponding to the NH groups, as well as the presence of the organic groups bonded to the tin atom in the complexes obtained from SnR_2Cl_2 . Moreover, in the complexes **1–11**, containing a 3-hydroxy-2-naphthohydrazone arm, the signal corresponding to the OH group is shifted to lower field due to the deshielding induced by deprotonation and coordination to tin that causes a greater electronic delocalization in the aromatic ring. On the other hand, the spectrum of complex **9** confirms the presence of one molecule of ethanol. The satellites corresponding to the coupling with tin can only be observed in the spectra of the methyl derivatives **1**, **4** and **7**. For these complexes substitution of $^2J(^{119}\text{Sn}-^1\text{H})$ values (55.9, 55.5 and 57.65 Hz respectively) into the corresponding Lockhart-Manders equation $\theta = 0.0161[{}^2J(^{119}\text{Sn}-^1\text{H})]^2 - 1.32[{}^2J(^{119}\text{Sn}-^1\text{H})] + 133.4$ (empirical relationship between the coupling constants and the C–Sn–C angle) [41] gives C–Sn–C angle values of 182.52, 181.81 and 185.68° which is in agreement with the axial disposition of the organic groups in an pentagonal bipyramid and is close to the value found in the crystal structures of complexes **4** (168.89°) and **7** (172.42°).

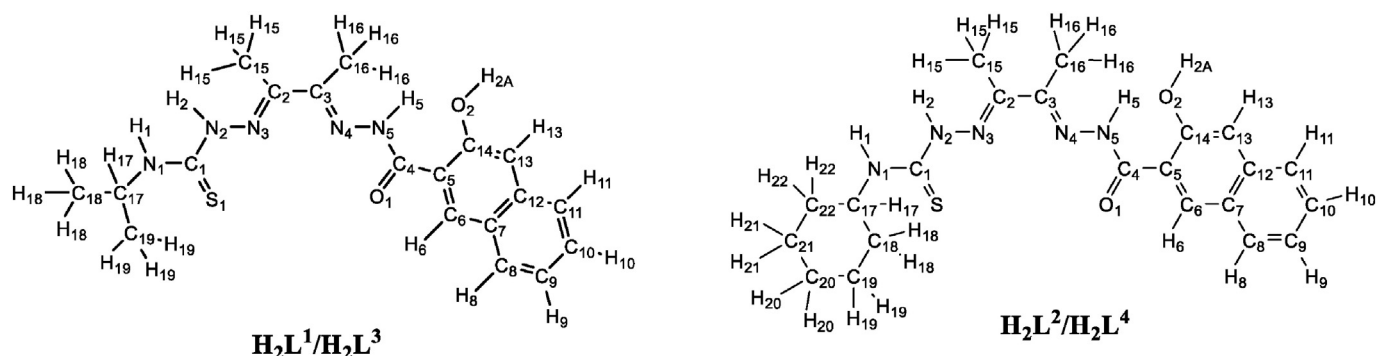


Fig. 8. Atom labelling used for the four ligands.

Table 4Chemical shifts (ppm) and coupling constants (Hz) observed in the ^1H NMR spectra of H_2L^1 , H_2L^2 , H_2L^3 , H_2L^4 and their tin complexes in DMSO- d_6 .

Compound	Organometallic	$\text{H}_{18}, \text{H}_{19}$	$\text{H}_{15}, \text{H}_{16}$	H_{17}	$\text{H}_9, \text{H}_{10}, \text{H}_{13}$	H_{11}	H_1^*, H_8	H_6	H_2	H_5	H_{2A}
H_2L^1		1.24, 6H, d 3J = 6.7	2.24, 3H, s 2.26, 3H, s	4.50, 1H, m	7.37, 2H, m 7.51, 1H, t 3J = 7.3	7.76, 1H, d 3J = 8.2	7.97, 2H, m	8.62, 1H, s	10.21, 1H, s	11.61, 1H, s	11.78, 1H, s
[SnMe $_2$ L 1] (1)	0.67, 6H, s 2J $_{(\text{Sn-H})}$ = 55.90	1.16, 6H, d 3J = 6.5	2.41, 3H, s 2.42, 3H, s	4.22, 1H, m	7.25–7.73, 4H*, m	7.73, 1H, d 3J = 8.7	7.93, 1H*, d 3J = 8.0	8.52, 1H, s	–	–	13.41, 1H, s
[SnBu $_2$ L 1] (2)	0.69, 6H, t 3J = 7.0 1.17, 12H, m	1.16, 6H, d 3J = 6.6	2.42, 3H, s 2.43, 3H, s	4.23, 1H, m	7.25–7.46, 4H*, m	7.73, 1H, d 3J = 8.1	7.92, 1H*, d 3J = 7.9	8.52, 1H, s	–	–	13.41, 1H, s
[SnPh $_2$ L 1 (OH $_2$)] (3)	7.58, 4H, d 7.15, 6H, m	1.18, 6H, d 3J = 6.5	2.39, 3H, s 2.40, 3H, s	4.28, 1H, m	7.31–7.48, 4H*, m	7.75, 1H, d 3J = 8.1	7.92, 1H*, d 3J = 8.1	8.57, 1H, s	–	–	13.07, 1H, s
H_2L^2		$\text{H}_{18} - \text{H}_{22}$ 1.17, 2H, m 1.36, 2H, m 1.68, 2H, m 1.87, 2H, m	2.16, 3H, s 2.23, 3H, s	4.17, 1H, s	7.36, 1H, t 3J = 6.8 7.51, 1H, t 3J = 6.7 7.36, 1H, s 7.30, 1H, t 3J = 6.8; 7.46, 1H, t, 3J = 6.9 7.24, 1H, s	7.75, 1H, d 3J = 8.4	7.88, 1H, s 7.96, 1H, d 3J = 8.5	8.62, 1H, s	10.24, 1H, s	11.60, 1H, s	11.76, 1H, s
[SnMe $_2$ (L 2)] (4)	0.66, 6H, s 2J $_{(\text{Sn-H})}$ = 57	1.12, 5H, m 1.25, 1H, m 1.70, 2H, m 1.92, 2H, m	2.41, 3H, s 2.42, 3H, s	3.86, 1H, s	7.30, 1H, t 3J = 6.8; 7.46, 1H, t, 3J = 6.9 7.24, 1H, s	7.77, 1H, d 3J = 8.2	7.27, 1H, s 7.92, 1H, d 3J = 8.4	8.52, 1H, s	–	–	13.40, 1H, s
[SnBu $_2$ (L 2)] (5)	0.68, 6H t 3J = 7.3 1.10, 7H, m, 1.24, 10H, m, 1.71, 2H, m 1.92, 2H, m		2.42, 3H, s 2.43, 3H, s	3.88, 1H, s	7.30, 1H, t 3J = 6 7.46, 1H, t, 3J = 6.9 7.25, 1H, s	7.73, 1H, d 3J = 8.6	7.29, 1H, s 7.92, 1H, d 3J = 8.6	8.52, 1H, s	–	–	13.41, 1H, s
[SnPh $_2$ (L 2)(OH $_2$)] (6)	7.09–7.20, 6H, m 7.58, 4H m	1.27, 4H, m 1.60, 1H, m 1.72, 2H, m 1.93, 2H, m	2.38, 3H, s 2.39, 3H, s	3.92, 1H, s	7.31, 1H, t 3J = 7.0 7.47, 1H, t 3J = 7.0 7.28, 1H, s	7.71, 1H, d 3J = 8.7	7.38, 1H, s 7.92, 1H, d 3J = 8.6	8.57, 1H, s	–	–	13.07, 1H, s
[Sn(L 2) $_2$] (10)	–	1.25, 5H, m 1.59, 1H, m 1.68, 2H, m 1.94, 2H, m	2.63, 3H, s 2.67, 3H, s	4.00, 1H, s	7.32, 1H, t 3J = 7.0 7.48, 1H, t 3J = 7.0 7.27, 1H, s	7.73, 1H, d 3J = 8.4	7.87, 1H, s 7.91, 1H, d 3J = 8.3	8.22, 1H, s	–	–	12.12, 1H, s
[SnL $_2$ (L 2)] (11)	–	1.15, 1H, m 1.32, 4H, m 1.62, 1H, m 1.74, 2H, m 1.93, 2H, m	2.59, 3H, s 2.64, 3H, s	4.06, 1H, s	7.40, 1H, s 7.56, 1H, t 3J = 7.0 7.40, 1H, s	7.82, 1H, d 3J = 8.5	7.84, 1H, s 8.06, 1H, d 3J = 8.3	8.49, 1H, s	–	–	11.40, 1H, s
H_2L^3					$\text{H}_9, \text{H}_{13}, \text{H}_{21}, \text{H}_{25}$ $\text{H}_{10}, \text{H}_{22}$ 7.33–7.49, 4H, m 7.49, 2H, t 3J = 6.9 7.33, 4H, m 7.49, 2H, t 3J = 6.9	H_{11} H_8 7.76, 2H, d 3J = 8.1 7.76, 2H, d 3J = 8.2 7.79, 2H, d 3J = 8.3	H_8 7.98, 2H, d 3J = 7.9 7.99, 2H, d 3J = 8.0 8.00, 2H, d 3J = 8.2	8.59, 2H, s	–	–	12.97, 2H, s 12.95, 2H, s 12.69, 2H, s
[SnMe $_2$ L 3] (7)	0.58, 6H, s 2J $_{\text{Sn-H}}$ = 57.65		2.60, 6H, s	–					–	–	12.97, 2H, s
[SnBu $_2$ (L 3)] (8)	0.64, 6H, t 3J = 7.0 1.15, 12H m,		2.55, 6H, s	–					–	–	12.95, 2H, s
[SnPh $_2$ L 3 (EtOH)] (9)	6.92–7.69, 10H, m		2.61, 6H, s	–	6.92–7.69, 12H, m				–	–	12.69, 2H, s
H_2L^4		$\text{H}_{18} - \text{H}_{22}$ 1.24–1.81, 20H, m	2.14, 6H, s	4.28, 2H, s			7.37, 1H, s		8.75, 1H, s	–	–
[SnL $_2$ (L 4)] (12)		1.34, 4H, m 1.65, 2H, m 1.78, 2H, m 2.13, 2H, m	2.63, 6H, s	4.04, 2H, s			5.57, 1H, s		–	–	–

The ^{13}C NMR spectra of the organic molecules show the signals expected for the proposed structures. In the ^{13}C NMR spectra of all the complexes (Table 5), the signals corresponding to the CN, CO and/or CS groups are shifted with respect to those of the free ligands, which indicate coordination through these groups, and therefore that the ligands act as tetradentate chelate donors.

It is known that ^{119}Sn NMR chemical shift depends on the coordination number and is also very sensitive to the type of donor atom bonded to the metal ion, so it is a useful tool to determine the chemical environment of the tin atom [42,43]. The ^{119}Sn NMR spectra were acquired both in DMSO solution and in the solid state (CP/MAS) and the chemical

shifts are summarized in Table 6. For complexes 1–9 the values found in DMSO solution correspond to seven-coordinated species due to the coordination of a solvent molecule or the replacement of the coordinated water molecule in complexes 3 and 6 and ethanol in complex 9. For the tin iodide derivative 10, the value falls within the range of other octa-coordinate tin(IV) compounds described in the literature [44]. Although complexes 11 and 12 have more negative values, the value corresponds well with N_2SOI_2 and $\text{N}_2\text{S}_2\text{I}_2$ environments respectively, where the presence of iodide leads to more negative values of the chemical shift, due to its high inductive effect and also to the possibility of additional π -contribution to the Sn–I bond, which would shield the

Table 5Chemical shifts (ppm) observed in the ^{13}C NMR spectra of H_2L^1 , H_2L^2 , H_2L^3 , H_2L^4 and their tin complexes in $\text{DMSO}-d_6$.

Compound	C ₁	C ₄	C ₁₄	C ₂ , C ₃	C ₁₂	C ₇	C ₆	C ₅	C ₈	C ₁₀	C ₁₁	C ₉	C ₁₃	C ₁₇	C ₁₈ –C ₁₉ /C ₂₂	C ₁₅ , C ₁₆	Organometallic
H₂L¹	177.2	161.7	153.0	148.6 148.3	136.3	133.1	129.5	128.9	127.7	126.2	124.4	121.1	111.2	46.3	22.2	12.1, 11.8	–
[SnMe ₂ L ¹] (1)	170.2	156.6		150.4	136.4	130.5	129.1	128.2	127.1	126.1	123.5	121.2	110.5	44.7	22.7	16.2, 15.5	18.8
[SnBu ₂ L ¹] (2)	170.3	156.7		150.9	136.5	130.4	129.2	128.0	127.1	126.1	123.4	121.3	110.5	44.7	22.7	16.2, 15.5	36.0, 27.5, 26.1, 14.1
[SnPh ₂ L ¹ (OH ₂)] (3)	170.7	156.5, 155.5		150.9	136.6	130.6	129.3	128.3	127.2	126.2	123.6	120.7	110.8	44.6	22.7	16.3, 15.7	133.8, 128.9, 128.2, 127.8
H₂L^{2*}	177.4	163.7	152.7	146.7	136.8	134.8	129.4	128.3	126.5	123.2	119.3	113.3	111.8	52.8	35.0, 26.8 13.8	16.6	–
[SnMe ₂ (L ²)] (4)	170.2	156.7		156.2	136.5	130.5	129.2	128.1	127.1	126.1	123.3	121.3	110.5	52.1	32.9, 25.8 19.7	16.2, 15.6	25.5
[SnBu ₂ (L ²)] (5)	170.3	156.7		Not observed	136.5	130.4	129.2	128.0	127.1	126.1	123.4	121.3	110.5	Not observed	32.8, 25.8 16.1	15.5, 14.1	36.0, 27.5, 26.1, 25.4
[SnPh ₂ (L ²)(OH ₂)] (6)	171.2	156.2	150.2	148.8	136.9	131.6	129.2	127.9	127.4	126.0	123.2	119.8	110.8	52.7	33.0, 25.6 24.9	16.8, 16.1	134.9, 129.4, 129.0, 128.6
[Sn(L ²) ₂] (10)	169.9	155.9		148.9	136.6	130.7	129.3	128.6	127.0	126.3	123.7	118.4	111.1	51.3	32.7, 25.6 25.1	16.2, 16.0	–
[SnL ₂ (L ²)] (11)	169.1	155.5		151.0	136.9	131.1	129.6	129.3	127.3	126.4	124.2	118.0	111.6	51.3	32.5, 25.6 19.0	17.0	–
H₂L^{3*}	160.8	152.8			136.6	133.7	129.4		127.7		124.8	118.9	111.8	–	–	12.7	–
[SnMe ₂ L ³] (7)	171.7	156.5		150.8	136.8	131.1	129.3	128.5	127.2	126.2	123.7	120.3	110.9	–	–	15.6	13.1
[SnBu ₂ L ³] (8)	172.0	156.5		151.3	136.8	131.0	129.3	128.5	127.2	126.2	123.7	120.3	110.9	–	–	15.5	30.8, 27.0, 26.0, 13.9
[SnPh ₂ L ³ (EtOH)] (9)	172.5	156.4		151.1 150.8	136.9	131.3	129.4	128.8	127.3	126.3	123.9	119.8	111.2	–	–	15.6	133.8, 128.7, 128.0
H₂L⁴	176.1	–		145.2	–									53.2	32.5, 25.4 24.6	10.6	–
[SnL ₂ L ⁴] (12)	169.3	–		142.7	–									52.8	33.9, 25.4 24.8	16.4	–

nucleus to a greater extent [45]. The chemical shifts found in the solid state for methyl (**1**, **4** and **7**) and *n*-butyl (**2**, **5** and **8**) derivatives are at least 100 ppm lower than the values found in solution, showing a decrease in the coordination number and correlate well with six-coordination. By contrast, the chemical shifts found in solution and in the solid state for the phenyl complexes (**3**, **6** and **9**) are similar and correspond to seven-coordination due to the presence of a water, ethanol or DMSO molecules. Substitution of sulfur by oxygen in the coordination sphere of the tin atom leads to a more negative chemical shift as a consequence of a decrease of the electronic density over the tin atom.

2.9. Antimicrobial activity

All the ligands and their corresponding diorganotin(IV) complexes were tested for antibacterial and antifungal activity (Table 7). In order to compare the results, the inhibitory effects of tin parent compounds SnMe₂Cl₂, SnBu₂Cl₂, SnPh₂Cl₂ and SnL₄ are also reported.

Table 6Chemical shifts (ppm) observed in the ^{119}Sn MNR spectra in $\text{DMSO}-d_6$ and in the solid state (CP/MAS).

Compound	DMSO- <i>d</i> ₆	CP/MAS
[SnMe ₂ L ¹] (1)	–399.8	–301.0
[SnBu ₂ L ¹] (2)	–380.2	–283.9
[SnPh ₂ L ¹ (OH ₂)] (3)	–516.8	–484.0
[SnMe ₂ L ²] (4)	–399.6	–240.3
[SnBu ₂ L ²] (5)	–379.9	–279.5
[SnPh ₂ L ² (OH ₂)] (6)	–378.5	–390.7
[SnMe ₂ L ³] (7)	–451.1	–293.9
[SnBu ₂ L ³] (8)	–454.3	–357.2
[SnPh ₂ L ³ H ₂ (EtOH)] (9)	–590.3	–571.5
[Sn(L ²) ₂] (10)	–789.4	–
[SnL ₂ L ²] (11)	–1072.2	–
[SnL ₂ L ⁴] (12) ^a	–1090.5	–

^a in CDCl₃.

Among the ligands, only **H₂L²**, with a mixed thiosemicarbazone/hydrazone structure and both cyclohexyl and naphthol rings, showed significant antibacterial properties against *S. aureus* at 12 $\mu\text{g mL}^{-1}$. Its dissymmetric analogous **H₂L¹**, with the presence of an isopropyl side chain instead of cyclohexyl, as well as the symmetric ligands diacetyl bis(3-hydroxy-2-naphthohydrazone) **H₂L³** and diacetyl bis(4-cyclohexyl-3-thiosemicarbazone) **H₂L⁴** were completely devoid of activity until the concentration of 200 $\mu\text{g mL}^{-1}$.

In this assay, some complexes exhibited antibacterial effect against Gram positive bacteria. The methyl derivative **1** was the most active, by inhibiting the growth of *B. subtilis* at the concentration of 6 $\mu\text{g mL}^{-1}$. This strain was also sensitive to the phenyl analogous **3** and to the methyl derivative of **H₂L²** **4** (MIC 200 $\mu\text{g mL}^{-1}$). In addition, these latest compounds, together with the phenyl and iodide complexes of **H₂L²** (**6** and **11** respectively), expressed a remarkable to moderate antibacterial activity towards *S. aureus* at concentrations ranging from 25 to 100 $\mu\text{g mL}^{-1}$, whereas a weak effectiveness was detected for **3** and **11** against *H. influenzae* Gram negative strain (MIC 200 $\mu\text{g mL}^{-1}$). Concerning antifungal properties of the new compounds, only a few chemicals were found to be active. Among these, complex **1** exhibited against *S. cerevisiae* MIC value of 200 $\mu\text{g mL}^{-1}$, and both complexes **11** and **6** inhibited the growth of *A. niger* at the concentrations of 100 and 200 $\mu\text{g mL}^{-1}$, respectively.

All the novel ligands and their complexes exhibited antimicrobial activity lower than that of ampicillin and miconazole, used, respectively, as antibacterial and antifungal positive controls.

The active compounds were also subjected to microbicidal susceptibility testing in order to elucidate the kind of their action. The results presented in Table 7 reveal that, in all cases, minimum bactericidal concentrations (MBCs) and minimum fungicidal concentrations (MFCs) are higher than the corresponding minimum inhibitory concentrations (MICs), suggesting a bacteriostatic and fungistatic behavior.

Compared to the parent organotin compounds tested here, the new complexes showed a decreased inhibition of the growth of both bacteria and fungi, with the exception of complexes **1** and **4** that, respectively,

Table 7Antimicrobial activity, expressed as MIC ($\mu\text{g mL}^{-1}$) and, in brackets, as MBC ($\mu\text{g mL}^{-1}$) and MFC ($\mu\text{g mL}^{-1}$).

Compound	Bacteria ^a				Fungi ^b		
	BS	SA	EC	HI	CT	SC	AN
H₂L¹	>200	>200	>200	>200	>200	>200	>200
[SnMe ₂ L ¹] (1)	6 (12)	>200	>200	>200	>200	200 (>200)	>200
[SnBu ₂ L ¹] (2)	>200	>200	>200	>200	>200	>200	>200
[SnPh ₂ L ¹ (OH ₂)] (3)	200 (>200)	25 (>200)	>200	200 (>200)	>200	>200	>200
H₂L²	>200	12 (>200)	>200	>200	>200	>200	>200
[SnMe ₂ L ²] (4)	200 (>200)	50 (>200)	>200	>200	>200	>200	>200
[SnBu ₂ L ²] (5)	>200	>200	>200	>200	>200	>200	>200
[SnPh ₂ L ² (OH ₂)] (6)	>200	100 (>200)	>200	>200	>200	>200	200 (>200)
[Sn(L ²) ₂] (10)	>200	>200	>200	>200	>200	>200	>200
[SnL ₂ L ²] (11)	>200	50 (>200)	>200	200 (>200)	>200	>200	100 (>200)
H₂L³	>200	>200	>200	>200	>200	>200	>200
[SnMe ₂ L ³] (7)	>200	>200	>200	>200	>200	>200	>200
[SnBu ₂ L ³] (8)	>200	>200	>200	>200	>200	>200	>200
[SnPh ₂ L ³ (EtOH)] (9)	>200	>200	>200	>200	>200	>200	>200
H₂L⁴	>200	>200	>200	>200	>200	>200	>200
[SnL ₂ L ⁴] (12)	>200	>200	>200	>200	>200	>200	>200
SnMe ₂ Cl ₂	50 (200)	200 (>200)	200 (>200)	200 (>200)	>200	100 (>200)	>200
SnBu ₂ Cl ₂	1.5 (12)	12 (50)	12 (50)	6 (25)	>200	200 (>200)	>200
SnPh ₂ Cl ₂	3 (25)	6 (25)	25 (100)	12 (50)	100 (>200)	50 (200)	12 (25)
SnI ₄	>200	>200	>200	>200	>200	>200	>200
Ampicillin	0.03 (0.3)	0.15 (0.7)	6 (12)	0.07 (0.3)	– ^c	–	–
Miconazole	–	–	–	–	3 (25)	12 (50)	3 (25)

^a Gram positive bacteria: *Bacillus subtilis* ATCC 6633 (BS) and *Staphylococcus aureus* ATCC 25923 (SA); Gram negative bacteria: *Escherichia coli* ATCC 8739 (EC) and *Haemophilus influenzae* ATCC 19418 (HI).^b Yeasts: *Candida tropicalis* ATCC 1369 (CT) and *Saccharomyces cerevisiae* ATCC 9763 (SC); mould: *Aspergillus niger* ATCC 6275 (AN).^c Not tested.

against *B. subtilis* (MIC 6 $\mu\text{g mL}^{-1}$) and *S. aureus* (MIC 50 $\mu\text{g mL}^{-1}$), were more potent than the starting SnMe₂Cl₂ (MIC 50 $\mu\text{g mL}^{-1}$ towards *B. subtilis* and 200 $\mu\text{g mL}^{-1}$ towards *S. aureus*). Furthermore, complex **11** also exhibited better effectiveness against *S. aureus* (MIC 50 $\mu\text{g mL}^{-1}$), *H. influenzae* (MIC 200 $\mu\text{g mL}^{-1}$) and *A. niger* (MIC 100 $\mu\text{g mL}^{-1}$) tested strains than the parent SnI₄ (MICs > 200 $\mu\text{g mL}^{-1}$).

In general, the presence of the mixed thiosemicarbazone/hydrazone structure plays a positive role in the antimicrobial properties of the newly synthesized compounds, whereas none of the symmetric bis(hydrazone) or bis(thiosemicarbazone) derivatives induced growth inhibition of the tested microorganisms.

Concerning the ligands, dissymmetric ligand **H₂L²**, expressed the best inhibitory effect that is due also to the presence of the cyclohexyl ring, because the change of this substituent by an isopropyl side chain led to inactive **H₂L¹**.

Similarly, the inhibitory effect of the complexes was found only for dissymmetric ligands bearing both thiosemicarbazone and hydrazone moieties, as well as methyl or phenyl organic groups or two iodido ligands bonded to the tin atom. The results obtained revealed that the active complexes show, in general, higher antimicrobial properties than the ligands. This behavior may be due to electron delocalization over the whole chelate rings, which increases the lipophilicity of the molecules and favors their permeation through the lipid layer of the microbial membranes [46], and also because of the biological effects of the organotin moieties impairing the normal cellular processes. Thus, the complexation of inactive **H₂L¹** led to methyl and phenyl complexes **1** and **3** that possess inhibitory effect against some bacteria and yeasts; in addition, **H₂L²** active derivatives **4**, **6** and **11** exhibited an antimicrobial spectrum wider than that of the ligand, unfortunately coupled

with a decreased inhibition of *S. aureus*. According to the data obtained in our study, the complexation reduced the antimicrobial activity of the starting organotin, owing to the introduction of a bulky organic structure strongly bonded to Sn. In this regard, the resulting complexes are comparatively less effective than the corresponding diorganotin precursors, except both **H₂L¹** and **H₂L²** methyl derivatives that exhibited enhanced antibacterial properties towards *B. subtilis* and *S. aureus* Gram positive strains. On the other hand, surprisingly, none of the butyl complexes exhibited activity, in spite of their lipophilic character higher than that of the methyl ones.

Concerning the antimicrobial pattern of the tin(IV) iodide derivatives, a significant increase in inhibition was observed for complex **11**, carrying two iodido ligands bonded to the tin atom, in comparison with the starting tin compound, whereas complex **10**, with the tin atom coordinated to two **H₂L²** ligands, was devoid of activity.

Conclusion

In this paper, we report the synthesis, characterization and *in vitro* antimicrobial properties of novel tetradentate ligands with two thiosemicarbazone/hydrazone functions and their tin(IV) complexes. The reactivity of the dissymmetric ligands strongly depends on the thiosemicarbazone used; while with cyclohexyl the ligand is stable under every reaction condition, with isopropyl quickly evolves to the obtaining of both symmetric derivatives. The coordination number of all the organometallic complexes is six, except in the case of the phenyl derivatives, in which it is seven, whereas the coordination numbers found in the reactions with tin(IV) iodide are six or eight. Mixed thiosemicarbazone/hydrazone ligand **H₂L²** and some of its organotin(IV) complexes, together with methyl and phenyl tin derivatives of **H₂L¹**, exhibited a certain inhibition of the

tested microorganisms. The highest activity was found against bacteria, being Gram positive *Bacillus subtilis* and *Staphylococcus aureus* the most sensitive microorganisms. Against these strains, especially the methyl complex of H_2L^1 and H_2L^2 ligand, respectively, demonstrated good antimicrobial efficacy. In contrast, both symmetric ligands H_2L^3 and H_2L^4 and all their resulting organotin(IV) complexes showed no effect.

Acknowledgements

The authors thank Dr. Josefina Perles from SIdI (UAM) for her kind help with the crystal refinement, to Instituto de Salud Carlos III, Ministerio de Economía y Competitividad (Spain) (Project PS09/00963) and Red de Excelencia MetalBio (CTQ2015-71211-REDT) for funding.

Appendix A. Supplementary data

Supplementary data to this article can be found online at <http://dx.doi.org/10.1016/j.jinorgbio.2016.07.002>.

References

- [1] J.S. Casas, M.S. García-Tasende, J. Sordo, *Coord. Chem. Rev.* 209 (2000) 197–261.
- [2] T.S. Lobana, R. Sharma, G. Bawa, S. Khanna, *Coord. Chem. Rev.* 253 (2009) 977–1055.
- [3] E. López-Torres, M.A. Mendiola, *Dalton Trans.* (2009) 7639–7647.
- [4] E. López-Torres, M.A. Mendiola, C.J. Pastor, B. Souto Pérez, *Inorg. Chem.* 43 (2004) 5222–5230.
- [5] A.M. Stadler, J. Harrowfield, *Inorg. Chim. Acta* 362 (2009) 4298–4314.
- [6] S. Naskar, M. Corbella, A.J. Blake, S.K. Chattopadhyay, *Dalton Trans.* (2007) 1150–1159.
- [7] P. Kumar, B. Narasimhan, *Mini Rev. Med. Chem.* 13 (2013) 971–987.
- [8] R. Narang, B. Narasimhan, S. Sharma, *Curr. Med. Chem.* 19 (2012) 569–612.
- [9] M.C. Rodríguez-Argüelles, P. Tourón-Touceda, R. Cao, A.M. García-Deibe, P. Pelagatti, C. Pelizzi, F. Zani, *J. Inorg. Biochem.* 103 (2009) 35–42 (and references therein).
- [10] A.G. Quiroga, C. Navarro Ranninger, *Coord. Chem. Rev.* 248 (2004) 119–133.
- [11] G.L. Parrilha, J.G. da Silva, L.F. Gouveia, A.K. Gasparoto, R.P. Dias, W.R. Rocha, D.A. Santos, N.L. Speziali, H. Beraldo, *Eur. J. Med. Chem.* 46 (2011) 1473–1482 (and references therein).
- [12] X. Shang, B. Zhao, G. Xiang, M.F.C. Guedes da Silva, A.J.L. Pombeiro, *RSC Adv.* 5 (2015) 45053–45060.
- [13] D.G. Calatayud, E. López-Torres, M.A. Mendiola, *Eur. J. Inorg. Chem.* (2013) 80–90.
- [14] D.G. Calatayud, E. López-Torres, J.R. Dilworth, M.A. Mendiola, *Inorg. Chim. Acta* 318 (2012) 150–161.
- [15] M.-X. Li, D. Zhang, L.-Z. Zhang, J.-Y. Niu, B.-S. Ji, *J. Organomet. Chem.* 696 (2011) 852–858.
- [16] N. Farrel, *Coord. Chem. Rev.* 232 (2002) 1–4.
- [17] M. Jain, S. Gaur, V.P. Singh, R.V. Singh, *Appl. Organomet. Chem.* 18 (2004) 73–82.
- [18] M. Gielen, M. Biesemans, R. Willen, *Appl. Organomet. Chem.* 19 (2005) 440–450.
- [19] M. Gielen, E.R.T. Tiekink (Eds.), *Metallotherapeutic Drug and Metal-Based Diagnostic Agents: 50 Tin Complexes and their Therapeutic Potential*, Wiley, New York, 2005.
- [20] S.A. Sadeek, M.S. Refat, H.A. Hashem, *J. Coord. Chem.* 59 (2006) 759–775.
- [21] T.S. Basu Baul, *Appl. Organomet. Chem.* 22 (2008) 195–204.
- [22] H. Yin, J. Li, M. Hong, J. Cui, L. Dong, Q. Zhang, *J. Mol. Struct.* 985 (2011) 261–269.
- [23] T. Sedaghat, M. Yousefi, G. Bruno, H. Amiri Rudbari, H. Motamedi, V. Nobakht, *Polyhedron* 79 (2014) 88–96.
- [24] F. Wang, H. Yin, J. Cui, Y. Zhang, H. Geng, M. Hong, *J. Organomet. Chem.* 759 (2014) 83–91.
- [25] A. Masia, S.V. Avery, M.A. Zorrodou, G.M. Gadd, *FEMS Microbiol. Lett.* 167 (2) (1998) 321–326.
- [26] A. Bonardi, C. Carini, Pelizzi, G. Pelizzi, G. Predieri, P. Tarasconi, M.A. Zorrodou, K.C. Molloy, *J. Organomet. Chem.* 401 (3) (1991) 283–294.
- [27] K.T. Mahmudov, M.F.C. Guedes da Silva, M.N. Kopylovich, A.R. Fernandes, A. Silva, A. Mizar, A.J.L. Pombeiro, *J. Organomet. Chem.* 760 (2014) 67–73.
- [28] D.H. Lloyd, *Vet. Dermatol.* 23 (2012) 299–304.
- [29] O. Megged, M. Assous, G. Weinberg, Y. Schlesinger, *Isr. Med. Assoc. J.* 15 (2013) 27–30.
- [30] K.W. McConeghy, D.J. Micolich, K.L. LaPlante, *Pharmacotherapy* 29 (2009) 263–280.
- [31] E. López-Torres, F. Zani, M.A. Mendiola, *J. Inorg. Biochem.* 105 (2011) 600–608.
- [32] A. Bacchi, A. Bonardi, M. Carcelli, P. Mazza, P. Pelagatti, C. Pelizzi, G. Pelizzi, C. Solinas, F. Zani, *J. Inorg. Biochem.* 69 (1998) 101–112 (and references therein).
- [33] G.M. Sheldrick, *SADABS Version 2.03*, Program for Empirical Absorption Corrections, Universität Göttingen, Göttingen, Germany, 1997–2001.
- [34] G.M. Sheldrick, *SAINT + NT (Version 6.04)* SAX Area-Detector Integration Program, Bruker AXS, Madison, WI, 1997–2001.
- [35] G.M. Sheldrick, *SHELXTL (Version 6.10)* Structure Determination Package, Bruker AXS, Madison, WI, 2000.
- [36] G.M. Sheldrick, *Acta Crystallogr. Sect. A* 46 (1990) 467.
- [37] J.H. Jorgensen, J.D. Turnidge, in: P.R. Murray, E.J. Baron, M.A. Pfaller, F.C. Tenover, R.H. Tenover (Eds.), *Manual of Clinical Microbiology*, American Society for Microbiology, Washington, DC 1999, pp. 1526–1554 (and 1640–1652).
- [38] J.P. Holland, F.I. Aigbihi, H.M. Betts, P.D. Bonnitcha, P. Burke, M. Christlieb, G.C. Churchill, A.R. Cowley, J.R. Dilworth, P.S. Donnelly, J.C. Green, J.M. Peach, S.R. Vasudevan, J.E. Warren, *Inorg. Chem.* 46 (2007) 465–485.
- [39] W.J. Geary, *Coord. Chem. Rev.* 7 (1971) 81–122.
- [40] E. López-Torres, A.L. Medina-Castillo, J.F. Fernández-Sánchez, M.A. Mendiola, *J. Organomet. Chem.* 695 (2010) 2305–2310.
- [41] T.P. Lockhart, W.F. Manders, *Inorg. Chem.* 25 (1986) 892–895.
- [42] B. Wrackmeyer in A.G. Davies, M. Gielen, K.H. Pannell, E.R.T. Tiekink (Eds.), *Fundamentals in tin chemistry, Tin chemistry: fundamentals, frontiers and applications*, Eds. Wiley, Weinheim, 2008, pp. 17–52.
- [43] H.C. Marsmann, F. Uhlig, in: Z. Rappoport (Ed.), *Further Advances in Germanium, Tin and Lead NMR, the Chemistry of Organic Germanium, Tin and Lead Compounds*, Wiley, Weinheim 2002, pp. 403–436.
- [44] E. López-Torres, A.R. Cowley, J.R. Dilworth, *Inorg. Chem. Commun.* 10 (2007) 724–727.
- [45] C. Pettinari, F. Marchetti, R. Pettinari, D. Martini, A. Drozdov, S. Troyanov, *Inorg. Chim. Acta* 325 (2001) 103–114.
- [46] R.S. Srivastava, *Inorg. Chim. Acta* 56 (1981) L65–L67.